Comparison between selective harmonic elimination and nearest level control for transistor clamped H-bridge inverter

Wail Ali Ali Saleh, Nurul Ain Mohd Said, Wahidah Abd Halim, Auzani Jidin
Research Laboratory of Power Electronic and Drive, Faculty of Electrical Engineering, Universiti Teknikal Malaysia Melaka, Malacca, Malaysia

Article Info

Article history:

Received Mar 14, 2021
Revised Feb 7, 2022
Accepted Feb 15, 2022

Keywords:

Modulation techniques
Multilevel inverters
Nearest level control
Newton Raphson method
Selective harmonic elimination
Total harmonic distortion
Transistor clamped H-bridge

ABSTRACT

Total harmonic distortion (THD) is a key index used to measure the quality of output waveforms in multilevel inverters. In this paper the THD is investigated and compared between two modulation methods; selective harmonic elimination and nearest level control, for 13-level transistor clamped H-bridge (TCHB) inverter. The selected TCHB topology employs a reduced number of DC sources and switches compared with other conventional multilevel inverters, which helps to reduce the size and cost of the inverter. The performance of both modulation methods has been validated through simulations using MATLAB/Simulink. The results show that for selective harmonic elimination, the 13-level output exists for a narrow range of modulation index, M $(0.687 \leq M \leq 0.694)$, while for nearest level control method, the 13-level output exists for a wider range of M $(M \geq 0.917)$, which means the 13-level output exists for different ranges of M for both methods. The THD obtained from both methods fulfills the IEEE Std 519-2014 standard of harmonics. Nearest level control method is conceptually simple and produces better THD results compared with selective harmonic elimination method.

Corresponding Author:

Nurul Ain Mohd Said
Research Laboratory of Power Electronic and Drive, Faculty of Electrical Engineering
Universiti Teknikal Malaysia Melaka
Hang Tuah Jaya, 76100 Durian Tunggal, Melaka, Malaysia
Email: nurulain@utem.edu.my

1. INTRODUCTION

Multilevel inverters (MLIs) [1]–[3] have gained a strong presence in the industry, particularly in medium and high power applications. MLIs offer several advantages when compared with two-level inverters, such as higher operating voltage capability, higher power quality, lower harmonic distortion and smaller filter size. Researchers are working hard to improve MLI topologies, control strategies and modulation techniques to reduce their size and cost and improve system reliability and efficiency. Harmonics are a very important factor to be considered when designing MLIs. Neglecting their effect may result in overheating and damage of electrical machinery as well as losses in the electrical system.

Recently, cascaded H-bridge (CHB) MLI has become one of the most popular MLIs due to its modular structure and efficiency. However, the CHB MLI requires separate DC power sources and a large number of switches, which makes the inverter too bulky. In contrast, the transistor clamped H-bridge (TCHB) MLI [4]–[6], generates a larger number of levels and requires fewer DC sources and switches. A single TCHB cell produces five levels at the output ($\pm V_{dc}$, $\pm 1/2\ V_{dc}$,0). The Reliability of TCHB MLI has been addressed in [7], in which the structure of TCHB has been modified to make it more reliable (fault-tolerant). Zhang *et al.* [8], a cost-effective approach based on a hybrid usage of silicon carbide (SiC) metal oxide semiconductor field effect transistors (MOSFETs) for some switches and silicon (Si) insulated-gate bipolar transistors (IGBTs) for other switches is proposed to improve the efficiency of TCHB MLI.

Based on the switching frequency, modulation techniques can be categorized into high switching frequency modulations and low switching frequency modulations. Switching frequency for multilevel inverters is considered high if it is above 1 kHz. High switching frequency modulations like multicarrier/ multireference PWM [9]–[12], space vector modulation (SVM) [13], [14] are superior in terms of harmonic minimization; however, they suffer from high switching losses. To overcome this issue, low switching frequency modulations are used. One of these modulations which has been widely investigated in the literature is the selective harmonic elimination (SHE) method [15]–[17]. The SHE method is capable of eliminating some low order harmonics. It is based on the solution of non-linear, transcendental equations representing the fundamental and harmonics components of the output waveform. Optimization techniques such as particle swarm optimization (PSO) [18] or iteration methods such as Newton Raphson (NR) algorithm [19], [20] are used to solve these equations. Another low switching frequency modulation is the nearest level control (NLC) [21]–[25]. NLC is based on selecting the nearest level to the reference. It is a simple method that can be easily extended to any number of levels without complicating the system.

This research work mainly focuses on applying SHE and NLC methods to 13-level TCHB inverter with equal DC sources and evaluating their performance in terms of THD reduction. The adopted TCHB MLI and the modulation methods applied to it are validated through simulations in MATLAB/Simulink. The THD results are analyzed and compared for both methods. It is expected that both methods fulfill the IEEE Std 519-2014 [26].

2. THE ADOPTED 13-LEVEL TCHB INVERTER

The 13-level TCHB inverter and its output waveform are shown in Figure 1. The power circuit of the inverter is shown in Figure 1(a). The configuration is composed of three identical TCHB cells which are fed by equal DC voltages. The output voltage waveforms of each TCHB cell and the overall 13-level inverter are shown in Figure 1(b). A representation of a single TCHB cell is shown in Figure 2, and its switching states are listed in Table 1.

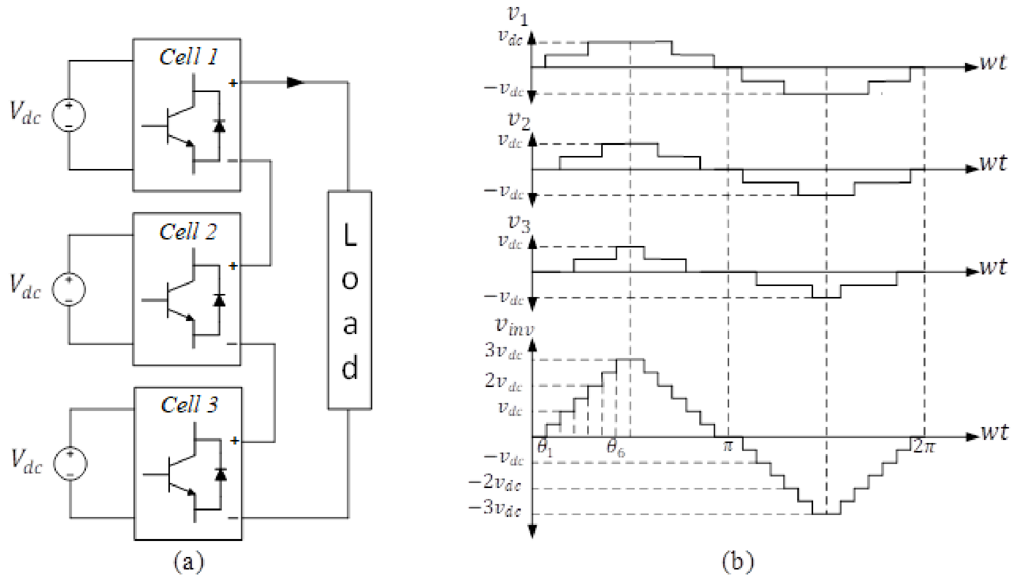

Figure 1. The 13-level TCHB inverter; (a) power circuit and (b) output voltages of cell-1, cell-2, cell-3, and the overall 13-level inverter

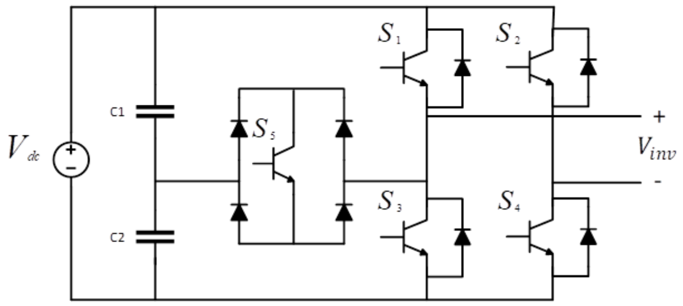

Figure 2. A single TCHB cell

Table 1. Switching states

No.	Switches ON	Voltage level
1	S_1, S_4	$+V_{dc}$
2	S_4, S_5	$+{}^{1}/_{2}\,V_{dc}$
3	S_1, S_2 or (S_3, S_4)	0
4	S_2, S_5	$-{}^{1}/_{2}\,V_{dc}$
5	S_2, S_3	$-V_{dc}$

It can be inferred that in the case of TCHB MLI, 15 switches are used to produce 13-level output, compared with 24 switches in the case of CHB MLI. To generate any output level, two switches in each TCHB cell must be switched on simultaneously (a total of six switches in all TCHB cells). The firing angles are alternatively selected in such a way that Cell-1 switches at θ_1 and θ_4, Cell-2 switches at θ_2 and θ_5, and Cell-3 switches at θ_3 and θ_6. The inverter output voltage is represented by the sum of the output voltages of all TCHB cells.

3. ANALAYSIS OF THE MULTILEVEL INVERTER OUTPUT VOLTAGE

In general, any periodic waveform can be represented using Fourier series expansion as (1).

$$V_{inv}(wt) = a_0 + \sum_{n=1}^{\infty}[a_n \cos(nwt) + b_n \sin(nwt)] \quad (1)$$

Because TCHB MLI output waveform is a quarter-wave symmetry, the coefficients a_0 and a_{n} are zeros for all n harmonics. So, the output voltage can be expressed as (2):

$$V_{inv}(wt) = \sum_{\mathrm{n}=1}^{\infty} b_n \sin(nwt) \quad (2)$$

where b_n represents the Fourier coefficients and can be described as (3):

$$b_n = \begin{cases} 0, & n = even \\ \frac{2v_{dc}}{n\pi}\sum_{i=1}^{s} cosn\theta_i, & n = odd \end{cases} \quad (3)$$

where s indicates the number of angles (steps) in a quarter wave, and θ_i represent the switching angles that should lie between 0 and ${}^{\pi}/_{2}$. The expression of the fundamental voltage V_1 is given by (4).

$$V_1 = b_1 = \frac{2V_{dc}}{\pi}[\cos(\theta_1) + \cos(\theta_2) + \cdots \cos(\theta_s)] \quad (4)$$

The voltage THD is given by (5).

$$THD = \sqrt{\sum_{n=2}^{\infty} V_n^2 / V_1^2} \quad (5)$$

4. SELECTIVE HARMONIC ELIMINATION METHOD

The basic principle of SHE method is to eliminate some significant low order harmonics and keep the fundamental voltage at the desired value. To perform that, the output waveform is decomposed into a number of equations that describe the fundamental and harmonics components as in (6):

$$\begin{aligned} &\cos(\theta_1) + \cos(\theta_2) + \cdots + \cos\theta_6 = sM \\ &\cos(3\theta_1) + \cos(3\theta_2) + \cdots + \cos(3\theta_6) = 0 \\ &\cos(5\theta_1) + \cos(5\theta_2) + \cdots + \cos(5\theta_6) = 0 \\ &\cos(n\theta_1) + \cos(n\theta_2) + \cdots + \cos(n\theta_6) = 0 \end{aligned} \quad (6)$$

where M is the modulation index and is given by (7).

$$M = \pi V_1 / 2sV_{dc} \qquad (0 \le M \le 1) \quad (7)$$

The set of equations in (6) are solved to obtain the optimized switching angles using NR method. This method starts with an initial guess of the switching angles and converges to the optimized solution after executing the method for several iterations. The execution of NR method is illustrated in the following steps [27]:

- Consider any arbitrary initial estimate for the switching angles ($\theta_1^0 - \theta_6^0$) which satisfy this condition ($0 < \theta_1 < \theta_2 < \cdots < \theta_6 < {}^{\pi}/_{2}$). Suppose: $\theta^0 = [\theta_1^0, \theta_2^0, \ldots, \theta_6^0\ ]^T$.
- Set the modulation index, M to 0.
- Calculate F(θ^0), $B(M)$ and Jacobian $J(\theta^0)$ matrices. where $F(\theta^0)=F^0$, $B(M) = [Ms, 0, 0, 0, 0, 0]^T$.
- Linearize about θ.

$$F^0 + [\partial F^0 / \partial \theta] \times\ d\theta^0 = B(M)$$

$$d\theta^0 = [d\theta_1^0\ d\theta_2^0\ d\theta_3^0\ \ldots\ d\theta_6^0]$$

- Compute the correction $d\theta^0$ during the iteration using the relation:

$$d\theta^0 = J^{-1}(\theta^0)(B(M) - \mathrm{F}(\theta^0))$$

where $J^{-1}(\theta^0)$ is the inverse matrix of $[\partial F^0 / \partial \theta]$

- Update the switching angles, i.e., $\theta(k+1) = \theta(k) + d\theta(k)$.
- Repeat steps (c) to (f) for several iterations until they satisfy the desired degree of accuracy.
- Increment *M* by a small, constant step.
- Repeat steps (b) to (h) for the whole range of M ($0 \le M \le 1$).
- Plot the obtained switching angles against M and then plot the voltage THD against M.

A MATLAB code is written to demonstrate NR method for the 13-level inverter. The results are shown in Figure 3. It was observed that the switching angles have a solution between *M*=0.687 and *M=0.694*, as depicted in Figure 3(a). Outside this range, the solutions either do not exist, or less than six angles are there, which is not applicable for the 13-level output. The voltage THD is calculated up to the 50th harmonic for the same range of M, as plotted in Figure 3(b). At $M = 0.691$, it is found that the minimum voltage THD is achieved and it is 6.8%. The angles at this point are 5.77°, 16.12°, 28.71°, 41.06°, 59.18° and 87.31°.

The process of generating gate signals for the TCHB MLI switches is implemented using comparators and logic gates. The comparison is made between a sinusoidal reference whose amplitude is considered to be 1 per unit and high and low voltage constants, $V_{h,p}$ and $V_{l,p}$, where p is the TCHB cell number. These voltage constants are based on the obtained switching angles and are given by (8).

$$\begin{aligned} &V_{l,p} = \sin(\theta_r) \quad , \quad r = 1, 3,5 \\ &V_{h,p} = \sin(\theta_z) \quad , \quad z = 2, 4,6 \end{aligned} \quad (8)$$

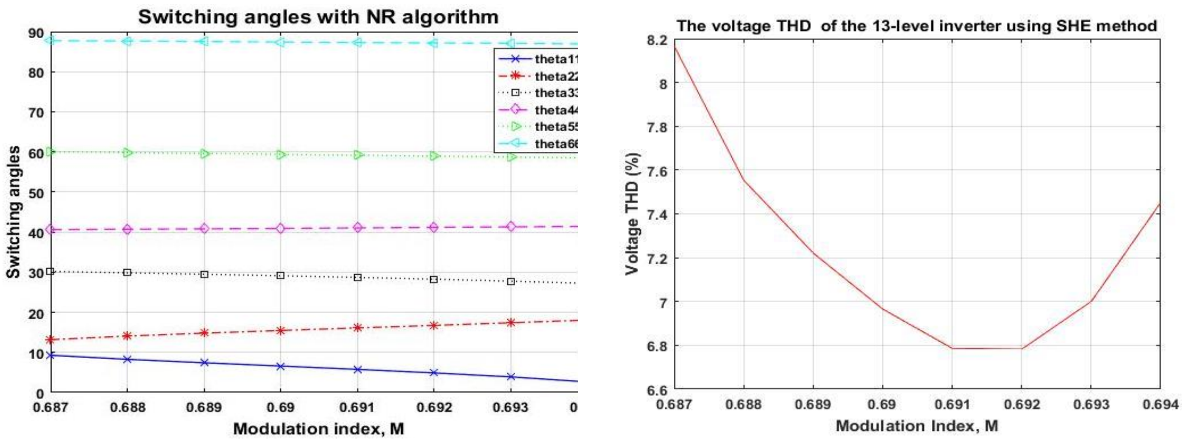

(a) (b)

Figure 3. MATLAB code results using SHE method; (a) Switching angles and (b) Voltage THD

5. NEAREST LEVEL CONTROL METHOD

NLC method, also called round method, is conceptually simple and straightforward. It simply compares the reference to the voltage levels and then selects the nearest level to the reference. Gate signals are then generated using comparators and basic logic gates and then fed to the inverter's switches. The round function is defined such that $round\ \{x\}$ is the integer closest to x. Figure 4 illustrates the NLC method. The application of NLC method to 13-level TCHB inverter is illustrated in Figure 4(a). First, the output is at zero level for an interval specified by the first switching angle. Then, the output switches to $0.5v_{dc}$ level when the reference reaches $0.25v_{dc}$. In the same way, when the reference reaches $0.75v_{dc}$, the output switches to v_{dc} level and so on. The control logic of NLC method for finding the nearest voltage level is illustrated in Figure 4(b). $V_{l,p}$ and $V_{h,p}$ are the constant values of comparison for the respected TCHB cell, p. In the case of 13-level output, the values of $V_{l,n}$ for the three cells are 0.083, 0.25, 0.416 and the values of $V_{h,n}$ are 0.583, 0.75 and 0.916, respectively. The reference amplitude is assumed to be 1 per unit.

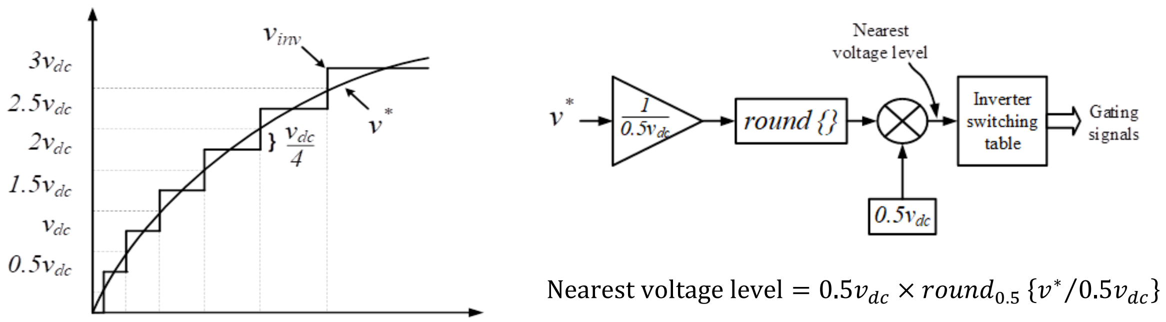

(a) (b)

Figure 4. NLC method; (a) Waveform synthesis and (b) Control diagram

The modulation index, M using NLC method can be calculated as in (9), where V_{ref} is the reference's amplitude. The switching angles of the 13-level TCHB inverter are calculated as in (10).

$$M = 2V_{ref}/s\,V_{dc} \tag{9}$$

$$\theta_i = sin^{-1}\left(\frac{i-0.5}{6M}\right), \qquad i = 1, 2, \dots, 6 \tag{10}$$

The 13-level output begins at $M = 0.917$, because according to the round method and as shown in Figure 4(a), if $3v_{dc}$ is considered as 1 per unit, the reference must reach $2.75v_{dc}$ or 0.917 per unit to generate

13-level output. Less number of levels is obtained when M is below 0.917. Using MATLAB code, the results of the NLC method are shown in Figure 5. The switching angles are calculated for a range of M from 0.92 to 1.15, as illustrated in Figure 5(a). The voltage THD is also calculated over the same range of M, as shown in Figure 5(b). It is noticed that the minimum THD is achieved at M=1.04, and it is equal to 5.09%. The switching angles at this point are 4.60°, 13.91°, 23.62°, 34.12°, 46.15° and 61.81°. In the overmodulation region, especially after $M = 1.04$, the voltage THD increases with the increase in M, and the output waveform will have a flat peak which gets wider with the increase in M.

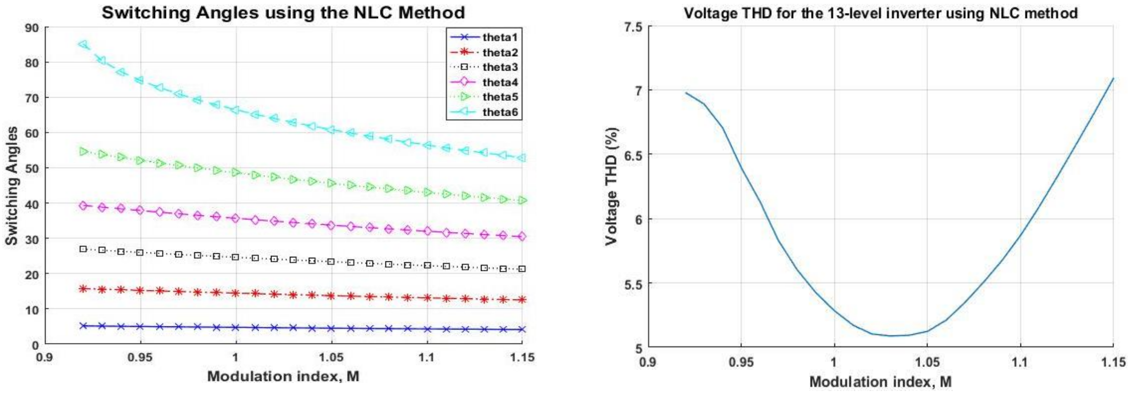

(a) (b)

Figure 5. MATLAB code results using NLC method; (a) Switching angles and (b) Voltage THD

6. SIMULATION RESULTS

The 13-level TCHB inverter along with the applied modulation methods are modelled through simulations in MATLAB/Simulink. Figure 6 shows a block diagram of the simulation model. The model consists of three identical TCHB cells. All TCHB cells are fed by equal DC voltages of 120V. Table 2 summarizes the specifications of the simulation parameters.

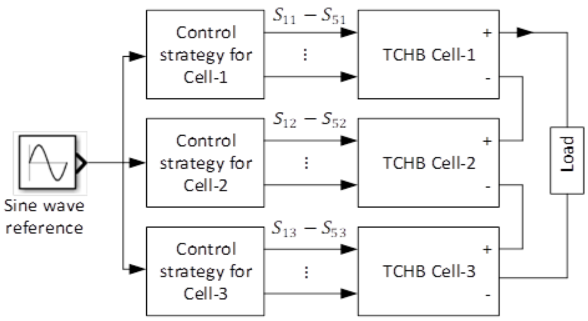

Figure 6. Block diagram of the 13-level TCHB inverter simulation

Table 2. Simulation parameters specifications

Parameter	Values
DC voltages	120V
DC-link capacitors	2200 uF
Load resistance	100 Ω
Fundamental frequency	50 Hz

6.1. Simulation results using SHE method

The simulation results using the SHE method at $M = 0.691$ are shown in Figure 7. Figure 7(a) depicts the output voltage of the 13-level inverter, where the peak voltage is 360V. Figure 7(b) demonstrates that the voltage THD is 7.11%, which is very close to the THD obtained from calculations with only 0.31%

difference. These results represent the minimum obtained voltage THD based on SHE method. It is observed that the low order odd harmonics up to the 11th harmonic have been almost eliminated. The simulation results at $M = 0.687$ (maximum THD) are shown in Figure 8. The output voltage waveform and its THD are shown in Figures 8(a) and (b), respectively, with voltage THD of 8.44%.

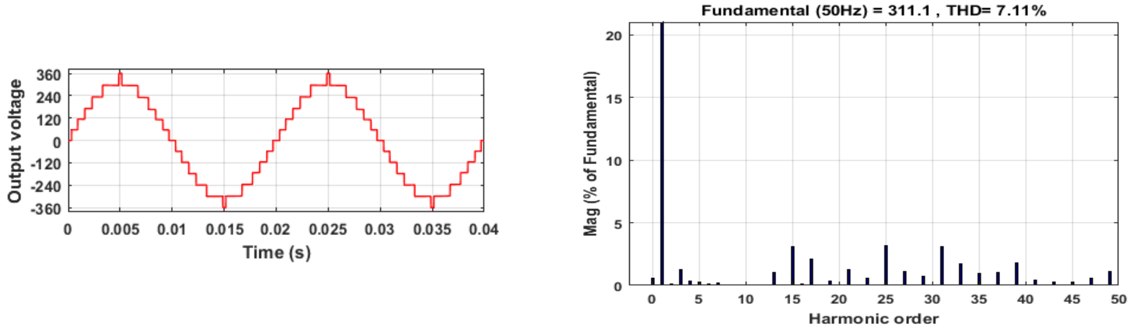

(a) (b)

Figure 7. Simulation results at $M = 0.691$; (a) Output voltage waveform and (b) Voltage THD

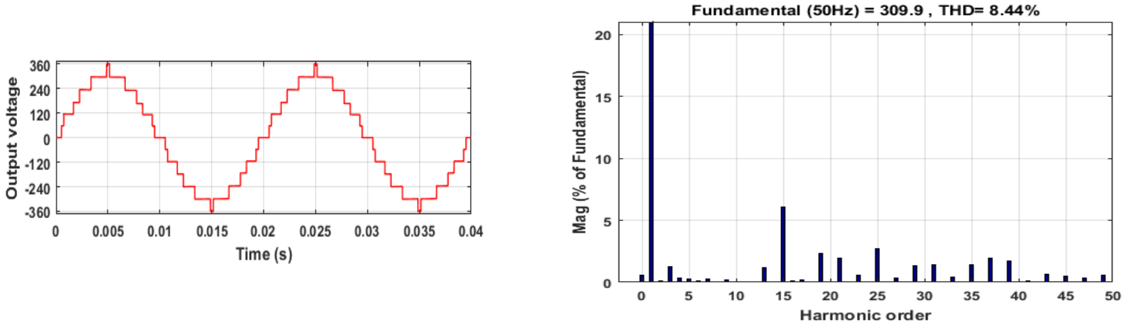

(a) (b)

Figure 8. Simulation results at $M = 0.687$; (a) Output voltage waveform and (b) Voltage THD

6.2. Simulation results using NLC method

The simulation results using NLC method at $M = 1.04$ are shown in Figure 9, where the output voltage of the 13-level TCHB inverter and its voltage THD spectrum are depicted in Figures 9(a) and (b), respectively. The voltage THD is equal to 5.18%, which approximately matches calculations with less than 0.1% difference. The result at $M = 1.04$ represents the minimum obtained voltage THD based on NLC method. The simulation results at $M = 0.92$ (maximum THD) are shown in Figure 10. The output voltage waveform and its THD are shown in Figures 10(a) and (b), respectively, with voltage THD of 7.11%.

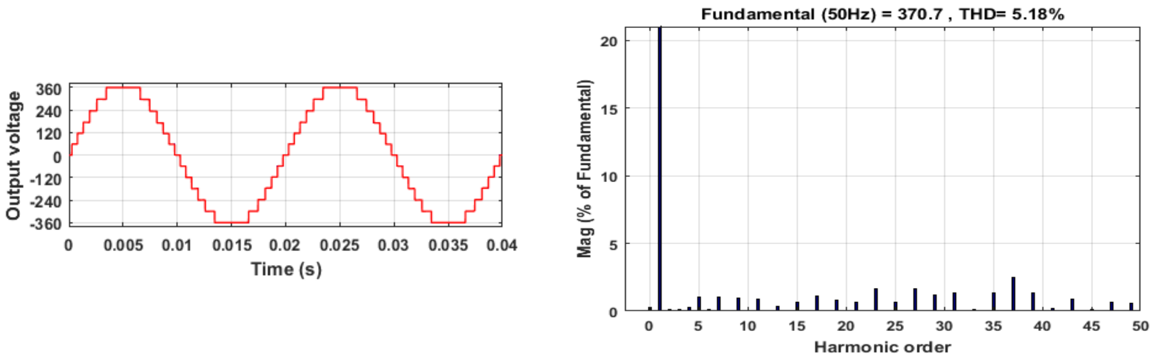

(a) (b)

Figure 9. Simulation results at $M = 1.04$; (a) Output voltage waveform and (b) Voltage THD

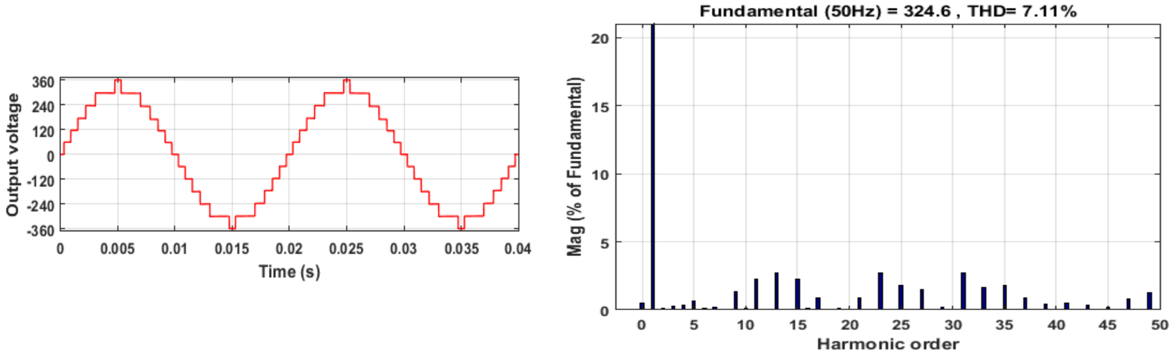

(a) (b)

Figure 10. Simulation results at $M = 0.92$; (a) Output voltage waveform and (b) Voltage THD

7. DISCUSSION

The main difference between NLC and SHE is that NLC reduces the overall THD of the output without eliminating certain harmonics; however, SHE eliminates some low order harmonics from the output waveform. When comparing the individual harmonics, it is clear that the 3rd, 5th, 7th, 9th and 11th harmonics have been almost eliminated in the case of SHE method. However, for NLC, the overall THD has been reduced without the focus on eliminating any individual harmonics. Another difference is that the voltage THD can be calculated using NLC method for a wide range of M ($M \geq 0.917$), whereas for SHE method, and using NR method, it can be calculated only for a narrow range of M ($0.687 \leq M \leq 0.694$). A comparison has been made between theoretical and simulation results of SHE and NLC methods at the minimum obtained voltage THD, as listed in Table 3. It can be seen that the minimum voltage THD occurs at different values of M for both mehods. It can also be noted that the NLC method achieves lower voltage THD results compared to the SHE method.

Table 3. Voltage THD comparison between NLC and SHE at minimum THD

Modulation method	SHE ($M = 0.691$)	NLC ($M = 1.04$)
Theoretical results	6.8%	5.1%
Simulation results	7.11%	5.18%

8. CONCLUSION

In this paper, SHE and NLC low switching frequency modulations were applied to 13-level TCHB inverter with equal DC voltage values. The voltage THD was investigated for different ranges of M as the 13-level output does not appear at the same range of M for both methods. NLC method operates for a wide range of M ($M \geq 0.917$), while SHE method operates for a narrow range of M ($0.687 \leq M \leq 0.694$). NLC achieves a lower voltage THD results compared to SHE. Finally, the voltage THD obtained from both methods fulfills the IEEE Std 519-2014, which allows an 8% THD limit for voltages less than 1kV.

ACKNOWLEDGEMENTS

This research work is sponsored under research grant FRGS/1/2020/F00417 from Universiti Teknikal Malaysia Melaka.

REFERENCES

[1] N. Prabaharan and K. Palanisamy, "A comprehensive review on reduced switch multilevel inverter topologies, modulation techniques and applications," *Renewable and Sustainable Energy Reviews*, vol. 76, no. December, pp. 1248–1282, 2017, doi: 10.1016/j.rser.2017.03.121.

[2] H. Akagi, "Multilevel Converters: fundamental circuits and systems," *Proceedings of the IEEE*, vol. 105, no. 11, pp. 2048–2065, Nov. 2017, doi: 10.1109/JPROC.2017.2682105.

[3] J. Rodriguez *et al.*, "Multilevel converters: An enabling technology for high-poer applications," *Proceedings of the IEEE*, vol. 97, no. 11, pp. 1786–1817, Nov. 2009, doi: 10.1109/JPROC.2009.2030235.

[4] A. Khergade, R. J. Satputaley, V. B. Borghate, and B. V. S. Raghava, "Harmonics reduction of adjustable speed drive using multi-objective dynamic voltage restorer," *2020 IEEE International Conference on Power Electronics, Smart Grid and Renewable Energy, PESGRE 2020*, no. September, 2020, doi: 10.1109/PESGRE45664.2020.9070589.

[5] R. J. Satputaley, V. B. Borghate, V. Kumar, and T. Kumar, "Experimental investigation of new three phase five level transistor clamped H-bridge inverter," *EPE Journal (European Power Electronics and Drives Journal)*, vol. 27, no. 1, pp. 31–42, 2017, doi: 10.1080/09398368.2017.1299505.

[6] S. J. Park, F. S. Kang, M. H. Lee, and C. U. Kim, "A new single-phase five-level PWM inverter employing a deadbeat control scheme," *IEEE Transactions on Power Electronics*, vol. 18, no. 3, pp. 831–843, 2003, doi: 10.1109/TPEL.2003.810837.

[7] S. P. Gautam, S. Gupta, and L. Kumar, "Reliability improvement of transistor clamped H-bridge-based cascaded multilevel inverter," *IET Power Electronics*, vol. 10, no. 7, pp. 770–781, 2017, doi: 10.1049/iet-pel.2016.0574.

[8] Y. Zhang, J. He, S. Padmanaban, and D. M. Ionel, "Transistor-clamped multilevel H-Bridge inverter in Si and SiC Hybrid configuration for high-efficiency photovoltaic applications," in *2018 IEEE Energy Conversion Congress and Exposition, ECCE 2018*, Sep. 2018, pp. 2536–2542, doi: 10.1109/ECCE.2018.8557394.

[9] S. Vinnakoti and V. R. Kota, "Performance evaluation of TCHB multilevel inverter with level-shifted PWM scheme," *Grenze International Journal of Electrical and Electronics Engineering* , Nov. 2015, pp. 21–31, 2015, doi: 10.3850/978-981-09-5247-1_006.

[10] Y. Babkrani, A. Naddami, and M. Hilal, "A smart cascaded H-bridge multilevel inverter with an optimized modulation techniques increasing the quality and reducing harmonics," *International Journal of Power Electronics and Drive Systems (IJPEDS)*, vol. 10, no. 4, pp. 1852-1862, 2019, doi: 10.11591/ijpeds.v10.i4.pp1852-1862.

[11] N. A. Rahim, M. F. M. Elias, and W. P. Hew, "Transistor-clamped H-bridge based cascaded multilevel inverter with new method of capacitor voltage balancing," *IEEE Transactions on Industrial Electronics*, vol. 60, no. 8, pp. 2943–2956, 2013, doi: 10.1109/TIE.2012.2200213.

[12] M. S. Bhaskar *et al.*, "Investigation of a Transistor clamped t-type multilevel H-Bridge inverter with inverted double reference single carrier PWM technique for renewable energy applications," *IEEE Access*, vol. 8, pp. 161787–161804, 2020, doi: 10.1109/ACCESS.2020.3020625.

[13] P. Jayal and G. Bhuvaneswari, "Space vector based enhanced modulation scheme for a reduced switch five-level inverter," *PIICON 2020 - 9th IEEE Power India International Conference*, pp. 1–6, 2020, doi: 10.1109/PIICON49524.2020.9112980.

[14] M. A. I. Al-Jewari, A. Jidin, S. A. A. Tarusan, and M. Rasheed, "Implementation of SVM for five-level cascaded H-bridge multilevel inverters utilizing FPGA," *International Journal of Power Electronics and Drive Systems*, vol. 11, no. 3, pp. 1132–1144, 2020, doi: 10.11591/ijpeds.v11.i3.pp1132-1144.

[15] M. Al-Hitmi, S. Ahmad, A. Iqbal, S. Padmanaban, and I. Ashraf, "Selective harmonic elimination in awide modulation range using modified Newton-raphson and pattern generation methods for a multilevel inverter," *Energies*, vol. 11, no. 2, 2018, doi: 10.3390/en11020458.

[16] M. Srndovic, A. Zhetessov, T. Alizadeh, Y. L. Familiant, G. Grandi, and A. Ruderman, "Simultaneous selective harmonic elimination and THD minimization for a single-phase multilevel inverter with staircase modulation," *IEEE Transactions on Industry Applications*, vol. 54, no. 2, pp. 1532–1541, 2018, doi: 10.1109/TIA.2017.2775178.

[17] M. Ahmed, A. Sheir, and M. Orabi, "Real-Time solution and implementation of selective harmonic elimination of seven-level multilevel inverter," *IEEE Journal of Emerging and Selected Topics in Power Electronics*, vol. 5, no. 4, pp. 1700–1709, Dec. 2017, doi: 10.1109/JESTPE.2017.2746760.

[18] A. K. Al-Othman and T. H. Abdelhamid, "Elimination of harmonics in multilevel inverters with non-equal dc sources using PSO," *Energy Conversion and Management*, vol. 50, no. 3, pp. 756–764, 2009, doi: 10.1016/j.enconman.2008.09.047.

[19] L. Manai, F. Armi, and M. Besbes, "Newton-raphson algorithm–based modified SHE for CHB multilevel inverter control considering capacitor voltage balancing and power factor variation," *International Transactions on Electrical Energy Systems*, vol. 29, no. 12, 2019, doi: 10.1002/2050-7038.12126.

[20] W. A. Halim, N. A. Rahim, and M. Azri, "Generalized selective harmonic elimination modulation for transistor-clamped H-bridge multilevel inverter," *Journal of Power Electronics*, vol. 15, no. 4, pp. 964–973, 2015, doi: 10.6113/JPE.2015.15.4.964.

[21] W. A. A. Saleh, N. A. M. Said, and W. A. Halim, "Harmonic minimization of a single-phase asymmetrical TCHB multilevel inverter based on nearest level control method," *International Journal of Power Electronics and Drive Systems*, vol. 11, no. 3, pp. 1406–1414, 2020, doi: 10.11591/ijpeds.v11.i3.pp1406-1414.

[22] M. I. Sarwar *et al.*, "A Hybrid nearest level combined with PWM control strategy: analysis and implementation on cascaded H-bridge multilevel inverter and its fault tolerant topology," *IEEE Access*, vol. 9, pp. 44266–44282, 2021, doi: 10.1109/ACCESS.2021.3058136.

[23] M. F. M. Elias, N. A. Rahim, H. W. Ping, and M. N. Uddin, "Asymmetrical cascaded multilevel inverter based on transistor-clamped H-bridge power cell," *IEEE Transactions on Industry Applications*, vol. 50, no. 6, pp. 4281–4288, 2014, doi: 10.1109/TIA.2014.2346711.

[24] M. Setti and M. Cherkaoui, "Low switching frequency modulation for generalized three-phase multilevel inverters geared toward Grid Codes compliance," *International Journal of Power Electronics and Drive Systems (IJPEDS)*, vol. 12, no. 4, p. 2349-2357, Dec. 2021, doi: 10.11591/ijpeds.v12.i4.pp2349-2357.

[25] N. A. M. Said, W. A. A. Saleh, and W. A. Halim, "Voltage harmonics reduction in single phase 9-level transistor clamped H-bridge inverter using nearest level control method," *Indonesian Journal of Electrical Engineering and Computer Science*, vol. 20, no. 3, p. 1725-1732, Dec. 2020, doi: 10.11591/ijeecs.v20.i3.pp1725-1732.

[26] IEEE Std 519, "IEEE Std 519-2014 (Revision of IEEE Std 519-1992), IEEE recommended practice and requirements for harmonic control in electric power systems," *IEEE Std 519-2014 (Revision of IEEE Std 519-1992)*, vol. 2014, pp. 1–29, 2014, doi: 10.1109/IEEESTD.2014.6826459.

[27] J. Kumar, B. Das, and P. Agarwal, "Selective harmonic elimination technique for a multilevel inverter," in *Fifteenth National Power Systems Conference (NPSC)*, 2008, pp. 608–613.

BIOGRAPHIES OF AUTHORS

Wail Ali Ali Saleh was born in Ibb, Yemen, in 1988. He received his B.Sc. degree in Electrical Engineering from University of Engineering and Technology, Taxila, Pakistan, in 2012. He has received his M.Sc. degree in Electrical Engineering from Universiti Teknikal Malaysia Melaka, UTeM, in 2021. His research interests include power converters, modulation techniques and FPGA. He can be contacted at email: wailali122@gmail.com.

Nurul Ain Mohd Said received the Ph.D. degree in electrical engineering from the University of New South Wales, Australia in 2017, and the M.Sc. from University of Strathclyde, Scotland in electrical power engineering with Business in 2009, respectively. She is currently with the Power Electronics and Drives Research Group at UTeM, Malacca, Malaysia. Her research interests include control of electrical machines, fault tolerant drive systems, and design of PM synchronous motor. She can be contacted at email: nurulain@utem.edu.my.

Wahidah Abd Halim received her B. Eng. degree (with Honors) in Electrical Engineering from the Universiti Teknologi Malaysia, Johor, Malaysia, in 2001. Her M.Sc. degree in Electrical Power Engineering from the Universiti Putra Malaysia, Selangor, Malaysia, in 2005 and her Ph.D. degree from the University of Malaya, Kuala Lumpur, Malaysia, in 2015. She is presently working as a Senior Lecturer in the Faculty of Electrical Engineering, Universiti Teknikal Malaysia Melaka. Her research interests include power electronics converters and FPGA applications. She can be contacted at email: wahidahhalim@utem.edu.my.

Auzani Jidin received the B. Eng., M. Eng. and Ph.D. degrees in power electronics and drives from Universiti Teknologi Malaysia, Johor Bahru, Malaysia, in 2002, 2004, and 2011, respectively. He is currently a Senior Lecturer with the Department of Power Electronic and Drive, Faculty of Electrical Engineering, Universiti Teknikal Malaysia Melaka, Melaka, Malaysia. His research interests include the field of power electronics, motor drive systems, field-programmable gate array, and DSP application. He can be contacted at email: auzani@utem.edu.my.